The Effect of Particle Size, Membrane Type, and Face Velocity on TiO_2-Containing Paint Dust Filtration

Adam W. Nored[1], Marie-Cecile G. Chalbot[2,3], Jin Y. Shin[4] and Ilias G. Kavouras[2,5]

[1] Interdisciplinary Engineering Program, School of Engineering, University of Alabama at Birmingham, Birmingham, 1075 13th St S, Birmingham, AL 35205, USA
[2] Department of Environmental Health Sciences, Ryals School of Public Health, University of Alabama at Birmingham, 1665 University Blvd, Birmingham, AL 35233, USA
[3] Department of Biological Sciences, School of Arts and Sciences, New York City College of Technology, 300 Jay St, Brooklyn, NY 11201, USA
[4] Department of Chemical and Environmental Sciences, School of Science, Health and Technology, CUNY Medgar Evers College 1638 Bedford Ave., Brooklyn, NY, 11225, USA
[5] Department of Environmental, Occupational and Geospatial Health Sciences, CUNY Graduate School of Public Health and Health Policy, 55 W 125th Street, New York, NY 10024, USA
* Corresponding author and E-mail: Ilias.Kavouras@sph.cuny.edu

ABSTRACT

The U.S. Centers of Diseases Control suggests the use filtering facepiece respirators (FFRs) for painters and related construction occupations. Engineered titanium dioxide (TiO_2) nanoparticles, shown to be more tumorigenic than bulk TiO_2, are prevalent in paint formulations. Specific occupational protection protocols are developed to manage tasks associated with TiO_2-containing paints and dust. In this study, the efficacy of different types of filtration membranes, namely, packed polypropylene (used in N95 FFRs), cellulose acetate, polycarbonate and polytetrafluoroethylene to remove paint dust containing TiO_2 nanoparticles was examined at various conditions. The particle mass size distribution of paint dust was measured using real-time 10-stage Quartz Crystal Microbalance (QCM) cascade impactor. Particles above 300 nm were more efficiently removed by cellulose acetate and polytetrafluoroethylene membranes. The filtration efficiency dropped rapidly for smaller particles in the 100-300 nm range. The results showed that the filtration efficiency of packed polypropylene membrane increased as particle size decreased with the highest computed for particles below 100 nm. This may be due diffusion by Brownian motion and electrostatic attraction. The low collection efficiency of cellulose acetate for the most penetrating and harmful particles below 100 nm was improved by increasing the face velocity. These results can be used by manufacturers to select materials for their respirators. The results can also facilitate future studies on the design and optimization of respirators using polypropylene or cellulose acetate membranes to remove the most potent TiO_2-containing ultrafine paint dust particles.

Keywords: Engineered TiO_2 nanoparticles, paint dust, ultrafine particles, N95 membrane, cellulose acetate

INTRODUCTION

Since 1973, occupational and environmental protections agencies such CDC, Occupational Safety and Health Administration (OSHA) and US Environmental Protection Agency (EPA) have been dealing with Pb-based paints consequences. Yet, an equally harmful and detrimental public health emergency may be brewing due to nanoparticles (NPs) containing paints (Muller *et al* 2018). TiO_2 is the most used white pigment in paints (ca. 70% of the total pigments) because of its high stability, anticorrosive and antibacterial properties. TiO_2 exists in different particle size fractions as fine particles (FPs) (diameter 0.1-2.5 µm) and nanoparticles (NPs) (diameter < 0.1 µm or 100 nm) (Ortlieb *et al* 2010). TiO_2 NPs embedded into paint may be less harmful because of agglomerate formation; however, the NPs are released upon degradation during weathering and sanding. The major exposure route of TiO_2 NP is inhalation in occupational settings. Sanding dust coated with nanoparticle containing paint was shown to be dominated by nano size particles (<300 nm) containing up to 80% TiO_2 and other NPs (Koponen *et al* 2015; Nored *et al* 2018).

Upon entry into the human body, TiO_2 NPs are absorbed and translocated across the air-blood barrier, distributed to organs and tissues by systemic circulation and interact with plasma–proteins, coagulation factors, platelets, and blood cells (Geiser *et al* 2010; Lee *et al* 2011; Eydner *et al* 2012). *In vivo* studies demonstrated the carcinogenic potential of TiO_2 NPs, with TiO_2 NPs being more tumorigenic than TiO_2 FPs on an equal mass dose basis (Trochimowicz *et al* 1988; Heinrich *et al* 1995). Owing to their relatively short time in use, early epidemiological studies did not detect an association between occupational exposure to TiO_2 particles and an increased lung cancer risk (Fryzek *et al* 2003). Moreover, the association of TiO_2 particle size, the most important determinant of TiO_2 NPs carcinogenicity, with lung cancer risk is not well studied. It is estimated that lifetime occupational exposures of TiO_2 NPs from 70 µg/m^3 to 700 µg/m^3 are associated with 0.1% excess risk of lung cancer (Dankovic *et al* 2007). Exposure and dose-response analysis across the lifecycle of products is seriously lacking for both occupational and environmental scenarios particularly in relation to particle size and processes generating high TiO_2 NP concentrations. It is, therefore, appropriate to control and mitigate TiO_2 NP exposures to reduce the burden on occupational health and safety, particularly for painters who already have a high prevalence of lung diseases, such as cancer (Lim et al., 2012), and chronic obstructive pulmonary disease (COPD) (Wang et al., 2016). Paint dust emissions are the ninth leading cause of disease in the coatings industry (Ringen et al., 2014).

The US OSHA recommended an exposure limit for TiO_2 NPs at 0.3 mg/m^3 (NIOSH 2011). TiO_2 NPs are also classified by the International Agency for Research of Cancer (IARC) as a Group 2B (possibly carcinogenic to humans) agent suggesting that products containing TiO_2 NPs should be managed cautiously (Baan 2007). Yet, more than 80% of workers and most consumers are not aware about the presence of NPs in paints (West *et al* 2016). Personal protective equipment such as N95 FFRs (i.e., removing at least 95% of particles 0.3 µm (or 300 nm) mass median aerodynamic diameter) have demonstrated poorer filtration of particles in 20-100 nm size range (may exceed 5%) with the most penetrating particle size at approximately 50 nanometers (Eninger *et al* 2008). Pre-charged fiber filters have the poorest protection from particles between 35-70 nanometers (Balazy *et al* 2005).

The goal of the study was to assess the efficiency of filtration membranes used for respiratory protection including polypropylene in N95 FFRs (i.e., designed to remove at least 95% of all airborne particles) to remove ultrafine paint dust particles containing engineered TiO_2 nanoparticles. In addition, the effects of particle size and face velocity was examined. Large porosity polycarbonate membrane was used to validate the role of porosity of particle filtration. Realistic TiO_2-containing paint dust was generated using a previously developed experimental apparatus (Nored *et al* 2017). Organic-based paint agglomerates included titanium dioxide NPs predominantly for particles with sizes < 100 nm. This was consistent with previous studies showing the accumulation of engineered NPs in ultrafine paint dust (Koponen *et al* 2011).

MATERIALS AND METHODS

Materials

A commercially available latex paint and primer formulation for indoor surfaces was used to coat wood panels. It was composed of water (49.6% w/w), non-volatile species (49.4% w/w), organic volatiles (0.9% w/w) and 2-amino-2-methyl-1-propanol (0.2% w/w) (CAS #: 124-68-5), TiO_2 (3.2% w/w) (CAS #: 13463-67-7), crystalline silica (0.22% w/w) (CAS #: 14808-60-7) and cristobalite (0.11% w/w) (CAS #: 14464-46-1). For abrasion, a BDERO600 2.4 Amp 5 inches (12.7 cm) orbital sander in its complete configuration (including the fitted filter) (Black & Decker, Towson, MD) fitted with Shopsmith® 5 inches (12.7 cm) aluminum oxide abrasive film discs with 120 grit (Shopsmith, Dayton, OH). The four membranes chosen were cellulose acetate (0.2µm pore size, 47-mm, Pall, MI), polytetrafluoroethylene (PTFE) (2.0µm, pore size, 47-mm, SKC Inc, PA), polycarbonate (Nuclepore®) (8 µm, pore size, 47-mm, Corning, NY) and polypropylene (N95, 3M 8210, St. Paul, MN).

Paint Dust Generation and Measurement

The Coatings Aerosol Resuspension System (CARES) was used to generate TiO_2 containing paint dust (Figure 1; Nored *et al* 2017). Briefly, paint dust polydisperse particles were generated from manually coated wood panels using an orbital sander in a polyvinylchloride glove box chamber (115 cm x 60 cm x 60cm) (Lancs Industries, Kirkland, WA). The efficiency of four membranes to collect TiO_2-containing paint dust was assessed by monitoring the size distribution of generated paint dust in the CARES (i.e., upstream) and after the membrane (i.e., downstream) for 5 min, simultaneously, and repeated at least six times (using a new wood panel each time) in order to get reproducible and accurate measurements. The collection efficiency of the four membranes was tested at face velocity of 1.92 cm/s. In addition, the collection efficiency of cellulose acetate membrane was measured at flow rates (Q: from 2 to 6 L/min) corresponding to face velocity of 1.92 to 5.76 cm/s and Reynolds number (Re) from 60 to 180.

The real-time 10-stage Quartz Crystal Microbalance (QCM) cascade impactor system (Model PC-2H, California, US) was used to measure particle mass in ten stages with 50% cut-off aerodynamic diameter cut-off points of 14, 9.7, 4.2, 2.8, 1.4, 0.7, 0.45, 0.30, 0.16 and 0.10 µm at 2 L/min flow rate. The average sensitivity is 1.4 ng per Hz but varies for each impactor stage because of differences in particle deposition in each stage. For typical ambient conditions, the signal-to-noise (S/N) ratio was more than 20, sufficient to adequately measure particle mass without crystal overloading. The impaction substrates (i.e., sensing crystals) were cleaned between experiments with n-hexane, and re-calibrated per manufacturer's protocol. In addition, the agreement between the two instruments was also assessed at the beginning and end of each experiment using indoor air for 15-20 minutes.

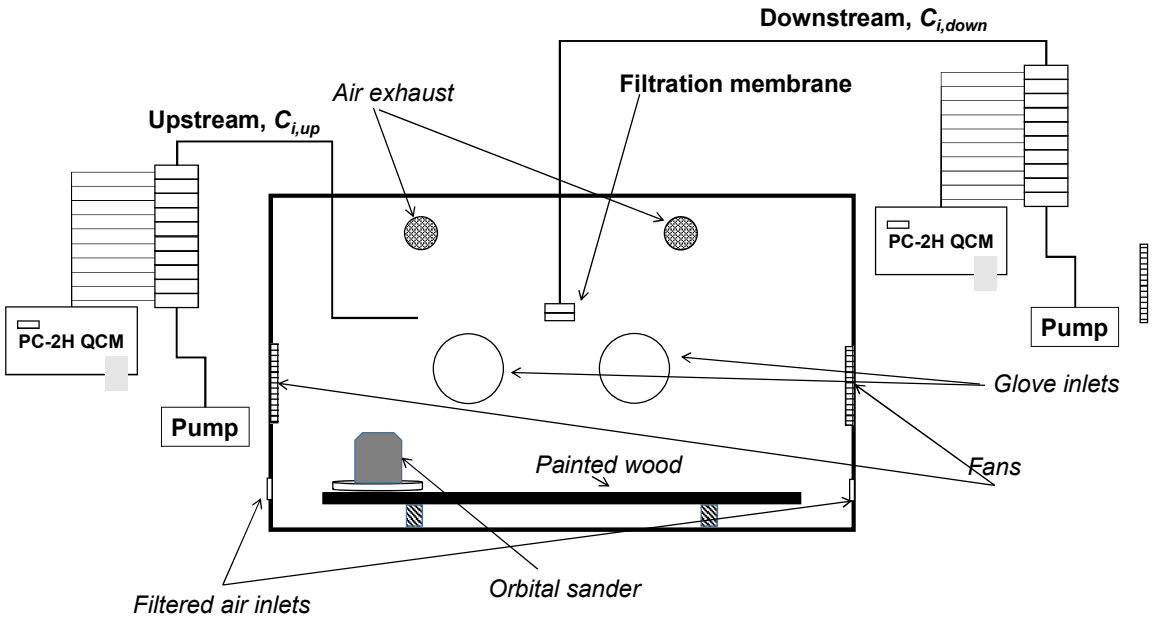

Figure 1. Schematic diagram of the experimental apparatus. Paint dust is generated into the chamber. The generated aerosol is measured in the chamber (Upstream, $C_{i,up}$) and after the filtration membrane (Downstream, $C_{i,down}$).

Total and size-dependent collection efficiency

The total (E_t) and size-dependent (E_i) collection efficiencies (dimensionless) were calculated using downstream ($C_{i,down}$) and upstream ($C_{i,up}$) particle mass concentrations as follows:

$$E_t = 1 - \frac{\sum_{i=1}^{10} C_{i,down}}{\sum_{i=1}^{10} C_{i,up}} \quad (1)$$

and

$$E_i = 1 - \frac{C_{i,down}}{C_{i,up}} \quad (2)$$

Statistical analysis

Particle mass concentrations were tested for normality using the Shapiro-Wilk test. The significance of difference in mean particle mass concentration values between groups was examined with the non-parametric Mann-Whitney (when two groups where compared) and Kruskal-Wallis (for more than two groups) tests at α=0.05. These tests were followed by Tukey's Honestly Significant Difference test. All analyses were done using SPSS (Version 25) (IBM Analytics, Armonk, NY) and Origin Pro (version 9.1) (OriginLab, Northampton, MA).

RESULTS

Figure 2 shows the representative relative size distribution of TiO_2-containing paint dust mass concentration in the CARES system (upstream) and after the cellulose acetate membrane (downstream). The total particle mass concentration was 540 ± 60 μg/m^3 for upstream and 17 ± 1 μg/m^3 for downstream ($p < 0.001$). The upstream concentration was comparable to that computed for paint dust using the same experimental configuration as previously (864 ± 503 μg/m^3; Nored *et al* 2018). Particles in the accumulation mode range (100 nm – 1.4 μm) accounted for most of the upstream paint dust mass (ca. 61%) but less than 35% of downstream paint dust mass. Note that particles with diameter < 100 nm account for a small fraction of particles by mass but their particle number concentration is 2-3 orders of magnitude higher than particles with diameter < 1 μm (Nored *et al* 2018).

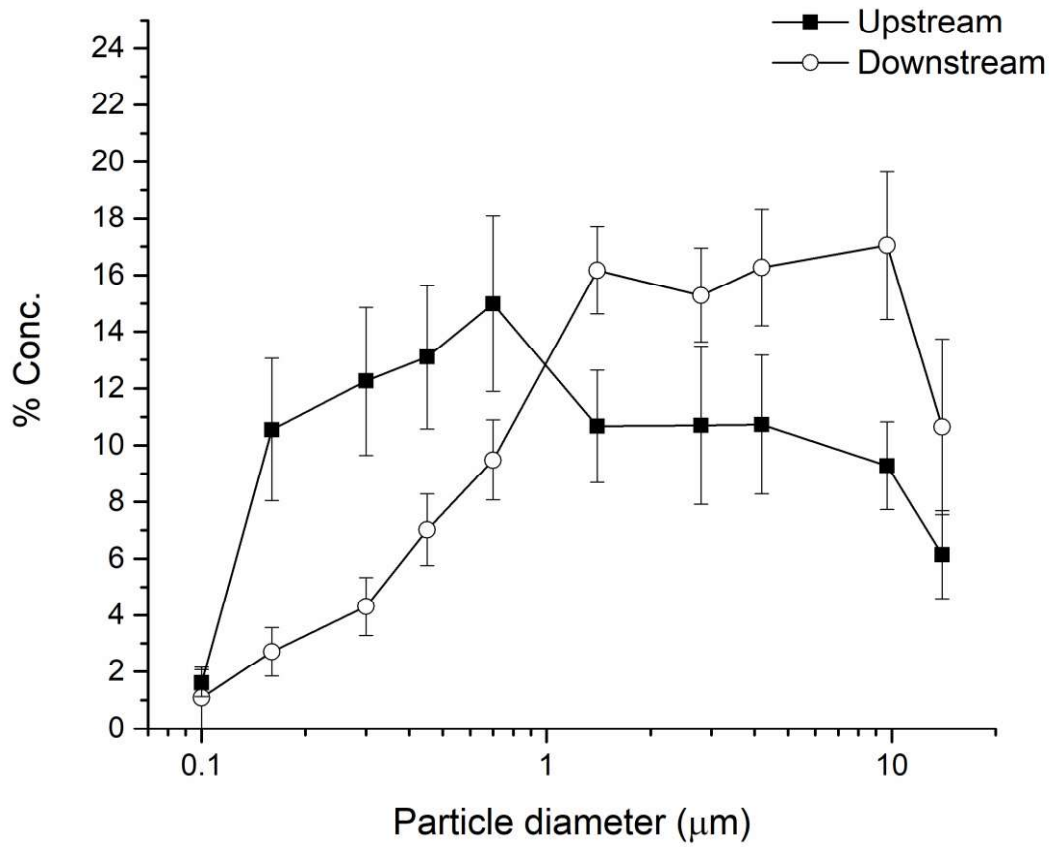

Figure 2. Percent relative mass (to the total particle mass) concentration of polydisperse paint dust aerosol upstream and downstream of cellulose acetate membrane at a face velocity of 1.92 cm/s in the CARES system. Squares and circles represent the average of at least six replicates of upstream and downstream concentration measured simultaneously. Error bars corresponds to 1.96 × standard error.

The collection efficiencies (E_t, dimensionless) as a function of particle size of each membrane at face velocity of 1.92 cm/s are shown in Figure 3. We compared polypropylene (the filter medium used for the NIOSH-recommended N95 FFRs), PTFE, and cellulose acetate membranes that are typically used for the collection of atmospheric aerosols. In addition, we also measured the collection efficiency of a porous polycarbonate membrane (pore size 8 µm). The polycarbonate membrane showed the poorest collection efficiency allowing for the penetration of most of the particles in the 0.45 – 9.7 µm size range (efficiencies varied from 11.6 % to 75%) due to its large pore size. Cellulose acetate and PFTE membranes filtered above 300 nm particles with efficiencies > 99% and rapidly declined for smaller particle sizes. In comparison, the filtration efficiency of N95 polypropylene membrane increased as particle size decreased with the highest efficiencies (i.e., 96-99%) computed for particles below 150 nm. Particles above 10 µm were less efficiently collected (90-95%) by all membranes.

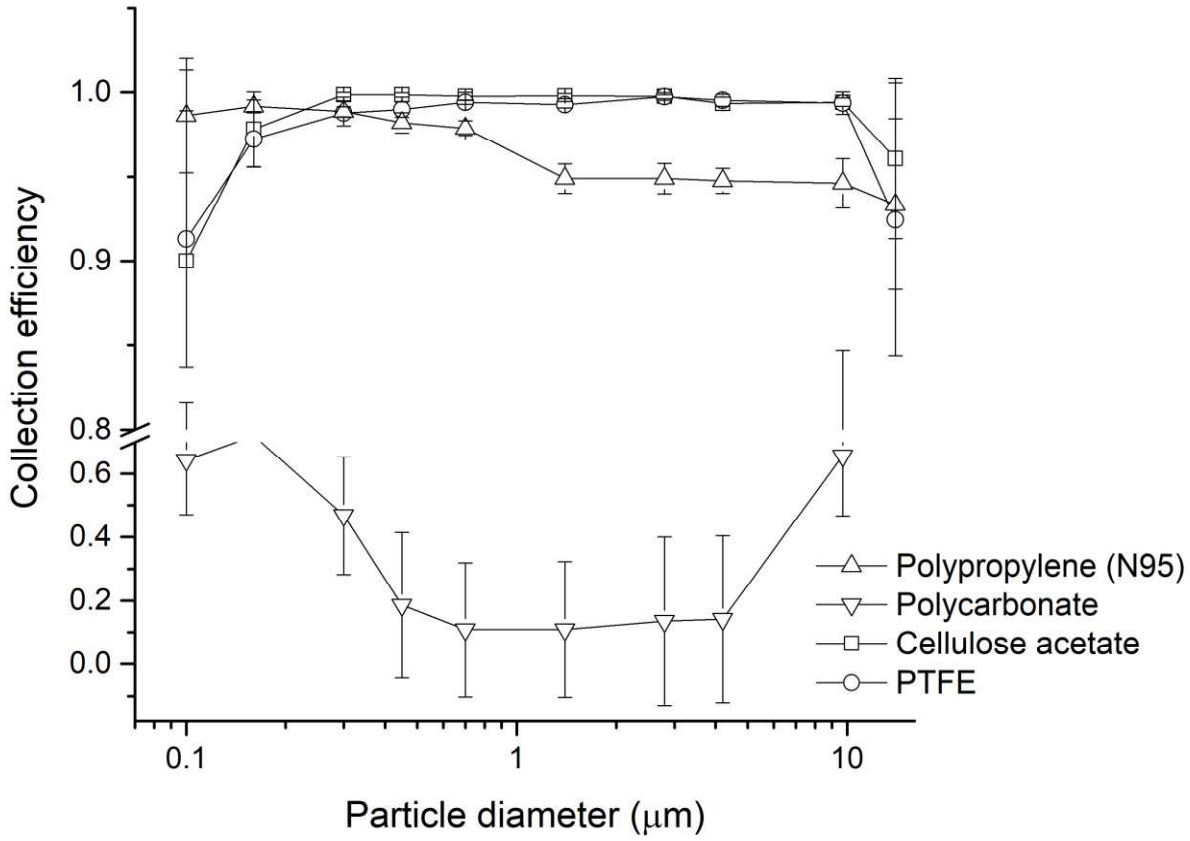

Figure 3. Collection efficiencies of polydisperse paint dust aerosol upstream and downstream of various membranes at a face velocity of 1.92 cm/s in the CARES system. Squares, circles, and triangles represent the average of at least six replicates of upstream and downstream concentration measured simultaneously. Error bars corresponds to 1.96 × standard error.

Table I summarizes the key findings of the efficiencies for all particles (E_t), and particles with diameter < 300 ($E_{<300}$) and < 100 ($E_{<100}$) nm of the membranes at different face velocities. Polypropylene membrane performed as designed to collect more than 95% of the particles above 300 nm (96.8% ± 18.8%), but also particles below 300 nm (98.9% ± 4.2%). The collection efficiencies of both cellulose acetate and PTFE membranes were superior (more than 99%) to that of polypropylene membranes for particles above and below 300 nm. However, the collection efficiencies for particles below 100 nm of cellulose acetate and PTFE membranes dropped to approximately 90% as compared to about 99% for polypropylene membranes.

Higher face velocities (3.84 and 5.76 cm/s) did not change the already high filtration efficiencies of particles above 300 nm but increased the filtration efficiency of particles below 100 nm up to 96.8% ± 18.8% at 3.84 cm/s and 96.8% ± 18.8% at 5.76 cm/s (Figure 4). Despite the increase, the other membranes were still inferior to the polypropylene membrane for the filtration of particles below 100 nm.

Table I. Filtration Efficiencies of Various Membranes at Flow Rates of 2, 4 and 6 L/min

Filter material	*Pore size*	*Q (L/min)*	*U (cm/sec)*	*% E_t*	*% $E_{<300}$*	*% $E_{<100}$*
Polypropylene (N95)	n/a	2.0	1.92	96.8 ± 18.8	98.9 ± 4.2	98.6 ± 1.2
Polycarbonate	8 µm	2.0	1.92	11.6 ± 38.3	64.1 ± 26.8	64.3 ± 8.2
Polytetrafluoroethylene	2 µm	2.0	1.92	99.5 ± 12.4	99.6 ± 8.4	91.3 ± 3.2
Cellulose acetate	0.2 µm	2.0	1.92	99.7 ± 16.0	99.6 ± 13.1	90.0 ± 4.7
Cellulose acetate	0.2 µm	4.0	3.84	99.1 ± 10.7	99.1 ± 5.3	93.6 ± 1.9
Cellulose acetate	0.2 µm	6.0	5.76	99.5 ± 1.6	99.2 ± 1.0	95.8 ± 3.6

DISCUSSION

Commercially available personal protective equipment (PPE), including N95 FFRs, are intended to efficiently remove airborne particles. The efficiency of the PPE depends on filtration variables such as face velocity, particle size, membrane material and porosity as well as the use-specific variables including proper fitting (i.e., the gap size between facial profiles and the PPE). Here, we examined the role of filtration variables on the efficiencies of various membranes to remove polydisperse particles of paint-dust, specifically those containing TiO_2 at < 100 nm (Nored *et al* 2018).

It has been shown that total filtration efficiency for particles above 600 nm was high for small pore-size, non-absorbent, hydrophobic thermoplastic polymer-based membranes (Akalin *et al* 2010). Inertial impaction and gravitation sedimentation may be the dominant mechanism for particles above 1 µm. The filtration efficiency for particles above 1 µm increased as face velocities increased, due to higher inertia. As particle size decreased from 1 µm to 100 nm, Brownian diffusion, and mechanical interception of particles by the filter fibers were the prevailing filtration mechanisms. Improved filtration efficiency may also be attributed to electrostatic attraction. The surface of TiO_2 NPs is found to be positive at pH less than 6.0 (Ramirez *et al* 2019) as compared to negatively charged PTFE and cellulose acetate (CH_3COO^-) membranes (He *et al* 2020). Polypropylene membranes are also considered electrostatic filters.

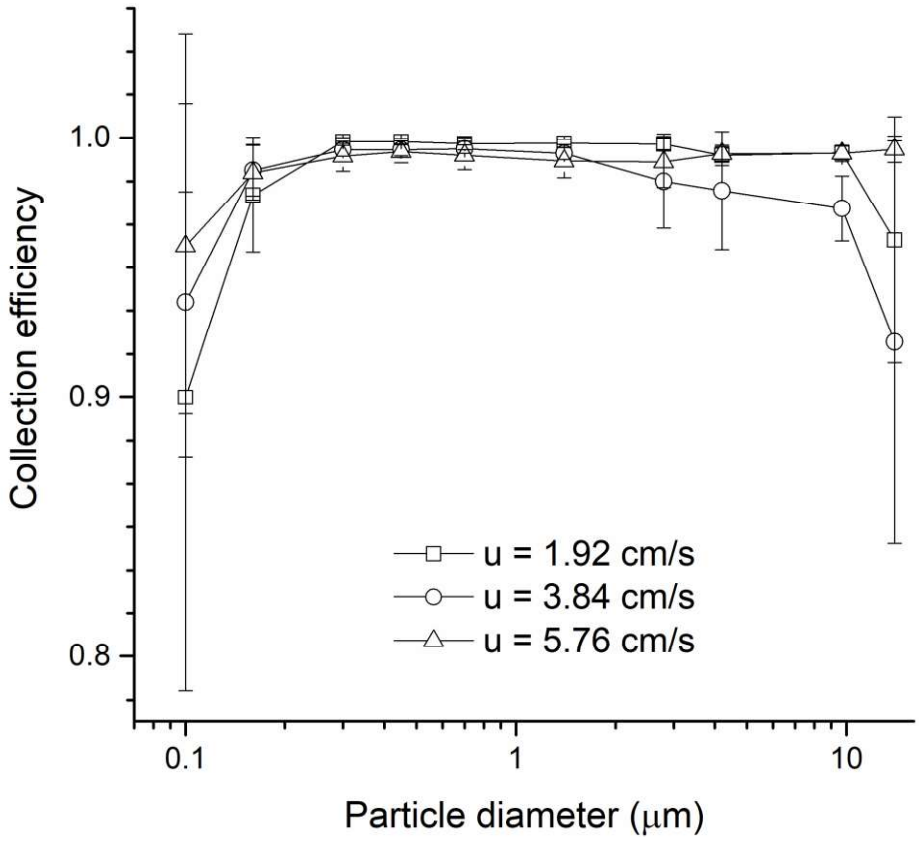

Figure 4. Collection efficiencies of polydisperse paint dust aerosol upstream and downstream of cellulose acetate at a face velocities of 1.92, 3.84 and 5.76 cm/s in the CARES system. Squares, circles, and triangles represent the average of at least six replicates of upstream and downstream concentration measured simultaneously. Error bars corresponds to 1.96 × standard error.

The filtration efficiency of particles below 300 nm was higher for PTFE and cellulose acetate than polypropylene membrane. The opposite was true for particles below 100 nm; the filtration efficiency of polypropylene membrane was higher than PTFE and cellulose acetate. This observation may be attributed to packing density, thickness, or fiber charge density in N95 FFRs polypropylene membranes as compared to thinner PTFE and cellulose acetate membranes (Huang *et al* 2013). It is noteworthy that diffusion and electrostatic attraction, the dominant mechanisms for the filtration of particles below 100 nm, differ for various conditions including face velocity and particle size, particularly in the nano-size range. For example, the electrostatic attraction is less effective as face velocity increases because of lower residence time (Givehchi *et al* 2015). The thermal rebound effect, i.e., the likelihood of particle detachment due to high thermal velocity and kinetic energy may further reduce the collection of particles below 100 nm at higher velocities. On the other hand, surface adhesion and elasticity, and the surface coating and potential to aggregate may limit thermal rebound and increase filtration efficiency for particles

below 100 nm (Warheit *et al* 2008). In addition, the filtration of particles below 100 nm increase over time due to filter loading. It has been shown that the capture of particles below 100 nm increases with increasing the loading time through the formation of dendrite crystals on single fibers (Bahloul *et al* 2014).

CONCLUSIONS

We have measured the filtration efficiencies of various commonly used membranes to filter paint dust particles containing TiO_2 NPs in the physiologically hazardous ~10 nm to 300 nm size range. We found that cellulose acetate and PTFE membranes efficiently filtered more than 99% of particles above 300 nm by mass, however their efficiency declined for particles below 100 nm. On the other hand, packed polypropylene membranes obtained from N95 masks showed filtration efficiencies slightly above 95% for particles above 300 nm, and higher filtration efficiency for particles below 300 and 100 nm. This may be attributed to the increased particle filtration by diffusion and electrostatic attraction in packed polypropylene membranes. The increase of the filtration efficiency of particles below 100 nm for PTFE and cellulose acetate membranes for higher face velocities may be due to the loading effect of previously collected particles in high concentration paint dust conditions.

REFERENCES

Akalin, M.; Usta, I.; Kocak, D.; Ozen, M.; (2010) Investigation of the filtration properties of medical masks. *Medical and Healthcare Textiles* 93-97.

Baan, R,A., (200&) Carcinogenic hazards from inhaled carbon black, titanium dioxide, and talc not containing asbestos or asbestiform fibers: recent evaluations by an IARC Monographs Working Group. *Inhalation Toxicology* 2007;19 Suppl 1:213-228.

Bahloul, A.; Mahdavi, A.; Haghighat, F.; Ostiguy, C., (2014) Evaluation of N95 filtering facepiece respirator efficiency with cyclic and constant flows. *Journal of Occupational and Environmental Hygiene* 11(8):499-508.

Bałazy, A.; Toivola, M.; Reponen, T.; Podgórski, A.; Zimmer, A.; Grinshpun, S.A., (2005) Manikin-based performance evaluation of N95 filtering-facepiece respirators challenged with nanoparticles. *Annals of Occupational Hygiene* 50, 259–269.

Dankovic, D.; Kuempel, E.; Wheeler, M., (2007). An approach to risk assessment for TiO2. *Inhalation Toxicology* 19, 205-212.

Eninger, R.M.; Honda, T.; Adhikari, A.; Heinonen-Tanski, H.; Reponen, T.; Grinshpun, S.A., (2008) Filter Performance of N99 and N95 Facepiece Respirators Against Viruses and Ultrafine Particles. *Annals of Occupational Hygiene*.52, 385–396.

Eydner, M.; Schaudien, D.; Creutzenberg, O.; Ernst, H.; Hansen, T.; Baumgärtner, W.; Rittinghausen, S., (2012) Impacts after inhalation of nano- and fine-sized titanium dioxide particles: morphological changes, translocation within the rat lung, and evaluation of particle deposition using the relative deposition index. *Inhalation Toxicology*, 24:9, 557-569, DOI: 10.3109/08958378.2012.697494

Fryzek, J.P.; Chadda, B.; Marano, D.; White, K.; Schweitzer, S.; McLaughlin, J.K.; Blot, W.J., (2003) A cohort mortality study among titanium dioxide manufacturing workers in the United States. *Journal of Occupational and Environmental Medicine* 45(4):400-409.

Geiser, M.; Kreyling, W.G., (2010) Deposition and biokinetics of inhaled nanoparticles. Particle Fibre Toxicology 7, 2. https://doi.org/10.1186/1743-8977-7-2

Givehchi, R.; Li, Q.; Tan, T., (2015) The effect of electrostatic forces on filtration efficiency of granular filters, *Powder Technology* 277, 135-140.

He, W.; Zhao, Y-B.; Jiang, F.; Guo, Y.; Gao, H.; Liu, J.; Wang, J., (2020) Filtration performance and charge degradation during particle loading and reusability of charged PTFE needle felt filters. *Separation and Purification Technology*, 233, 116003.

Heinrich, U.; Fuhst, R.; Rittinghausen, S.; Creutzenberg, O.; Bellmann, B.; Koch, W.; Levsen, K., (1995) Chronic Inhalation Exposure of Wistar Rats and two Different Strains of Mice to Diesel Engine Exhaust, Carbon Black, and Titanium Dioxide, *Inhalation Toxicology*, 7:4, 533-556.

Huang, S.-H; Chen, C.-W.; Kuo, Y.-M.; Lai, C.-Y.; McKay, R.; Chen, C.-C., (2013) Factors affecting filter penetration and quality factor of particulate respirators. *Aerosol and Air Quality Research* 13(1), 162-171.

Koponen, I.M.; Jensen, K.A.; Schneider, T., (2011) Comparison of dust released from sanding conventional and nanoparticle-doped wall and wood coatings. *Journal of Exposure Science and Environmental Epidemiology 21*:408–418.

Lee, J. H.; Kwon, M.; Ji, J. H.; Kang, C. S.; Ahn, K. H.; Han, J. H.; Yu, I. J., (2011). Exposure assessment of workplaces manufacturing nanosized TiO2 and silver. *Inhalation Toxicology*, 23(4), 226–236.

Lim, S.S.; Vos, T.; Flaxman, A.D.; Danaei, G.; Shibuya, K.; Adair-Rohani, H., (2012) A comparative risk assessment of burden of disease and injury attributable to 67 risk factors and risk factor clusters in 21 regions, 1990–2010: a systematic analysis for the Global Burden of Disease Study. *Lancet* 380(9859):2224–2260.

Muller, C.; Sampson, R.J.; Winter, A.S., (2018) Environmental Inequality: The Social Causes and Consequences of Lead Exposure. *Annual Review of Sociology* 44:1, 263-282.

NIOSH. Current Intelligence Bulletin 63. Cincinnati: National Institute for Occupational Safety and Health; 2011. Occupational Exposure to Titanium Dioxide.

Nored, A.W.; Chalbot, M.C-C.G.; Kavouras, I.G., (2018) Characterization of paint dust aerosol generated from mechanical abrasion of TiO2-containing paints, *Journal of Occupational and Environmental Hygiene* 15:9, 629-640, DOI: 10.1080/15459624.2018.1484126.

Ortlieb, M., (2010). White Giant or White Dwarf?: Particle Size Distribution Measurements of TiO2. *GIT Laboratory Journal Europe*, 14, 42-43.

Ramirez, L.; Ramseier Gentile, S.; Zimmermann, S.; Stoll, S., (2019) Behavior of TiO_2 and CeO_2 Nanoparticles and Polystyrene Nanoplastics in Bottled Mineral, Drinking and Lake Geneva Waters. Impact of Water Hardness and Natural Organic Matter on Nanoparticle Surface Properties and Aggregation. *Water 11*, 721. https://doi.org/10.3390/w11040721

Ringen, K.; Dement, J.; Welch, L.; Dong, X.S.; Bingham, E.; Quinn, P.S.,(2014) Risks of a lifetime in construction. Part II: Chronic occupational diseases. *American Journal of Industrial Medicine* 57(11):1235–45.

Trochimowicz, H.J.; Lee, K.P.; Reinhardt, C.F., (1988). Chronic inhalation exposure of rats to titanium dioxide dust. *Journal of Applied Toxicology*, 8:383–385.

Wang, X.; Dong, X.S.; Welch, L.; Largay, J.; (2016) Respiratory Cancer and Non-Malignant Respiratory Disease-Related Mortality among Older Construction Workers-Findings from the Health and Retirement Study. *Occupational and Medical Health Affairs* 4:235.

Warheit, D.B.; Sayes, C.M.; Reed, K.L.; Swain, K.A., (2008) Health effects related to nanoparticle exposures: environmental, health and safety considerations for assessing hazards and risks. *Pharmacology & Therapeutics* 120(1), 35-42.

West, G.H.; Lippy, B.E.; Cooper, M.R.; Marsick, D.; Burrelli, L.G.; Griffin, K.N.; Segrave, A.M., (2016) Toward responsible development and effective risk management of nano-enabled products in the U.S. construction industry. *Journal of Nanoparticle Research* 18(2), 1-27.